

Dependence of Anomalous REG Performance on Run Length

ROBERT G. JAHN AND YORK H. DOBYNS

*Princeton Engineering Anomalies Research Laboratory
School of Engineering and Applied Science
Princeton University, Princeton, NJ 08544
e-mail: rgjahn@princeton.edu*

Abstract—In random event generator (REG) experiments yielding anomalous results, any evolution of effect sizes over extended runs of data collection could, in principle, give some insight into the fundamental mechanism of the binary probability distortions. Retrospective examination of large individual and collective databases acquired over many years of previous study proves only marginally capable of distinguishing any such functional dependence on run length from a constant effect size model, which does little to narrow the phenomenological possibilities. However, an unanticipated ancillary feature of this data treatment is the emergence of a suggestively small blockwise variance in the anomalous effect sizes, possibly indicative of sequential correlations in the data streams that are not present in the baseline data. If real, such correlations would imply that the mechanism of the anomalous effect is more complicated than a simple change of elementary binary probabilities, although the set of possible models is so large that no specific inference can be drawn at this time.

Keywords: consciousness—human machine anomalies—random event generator (REG)

I. Introduction

Most electronic random event generators (REGs) used in research on consciousness-related anomalies convert some primary form of conduction electron thermal noise into secondary random strings of binary pulses suitable for systematic accumulation and counting.^(1,2) Properly designed and constructed, such devices in nominal operation produce output digital data that cumulate to the theoretical binomial distribution for binary probability $p = 0.5$. For a sufficiently large number of samples this is well approximated by the normal Gaussian distribution,

$$n(c) = \frac{N}{\sqrt{2\pi\sigma}} e^{-\frac{1}{2}\left[\frac{c-\mu}{\sigma}\right]^2} \quad (1)$$

where $n(c)$ is the number of sample counts of value c , N the total number of samples taken, μ the mean value of the distribution, and σ its standard deviation. For $p = 0.5$, μ and σ take the following values:

$$\mu = pN = \frac{N}{2} \quad (2)$$

$$\sigma = \sqrt{p(1-p)N} = \frac{\sqrt{N}}{2}. \quad (3)$$

In the simplest experimental applications, human operators are asked to influence these devices to produce higher than chance values of μ (HI); lower than chance values (LO); or chance (baseline) values (BL), in an interspersed tripolar protocol. These results are then compared with each other, with calibration data, and with theoretical expectations to compute statistical figures of merit for any apparently anomalous behavior. The most direct indicators of aberrations in the output strings are shifts in the means of their count distributions, $\Delta\mu$. These can be instructively displayed as cumulative deviation graphs of the $\Delta\mu$, as a function of the number of samples collected. The theoretically anticipated behavior of such displays, which should be verified by empirical calibrations of the devices, is simply a one-dimensional binary random walk, as sketched in Figure 1, trace C. Note that while the expected mean value of $\Delta\mu$ remains at zero, the anticipated excursions of the cumulative $\Delta\mu$ about this value increase as the prevailing standard deviation, *i.e.*, proportional to \sqrt{N} .

In contrast to this chance behavior, the results of “successful” active experiments typically display the same character of stochastic progression, but now superimposed on secular drifts toward positive, or negative, values of cumulative $\Delta\mu$, in correlation with the pre-recorded intentions of the operators (Figure 1, traces HI and LO). Baseline intention results tend to conform more closely to the chance expectations, but can display subtler aberrations of their own.^(3,4)

The most parsimonious interpretation of such empirical behavior is that the operator influence manifests as a small change in the intrinsic binary probability of the bit-wise events that are being counted, Δp , which shifts the running mean values of the distributions by an amount $\Delta\mu = \Delta pN$. In other words, the experimental behavior continues to conform to chance distributions, but now for binary samples of slightly increased, or decreased, intrinsic probabilities. More detailed analyses of the overall shape of the data distribution functions have supported this model of the anomalous effects at subtler structural levels as well.⁽⁵⁾ None of these assessments, however, are competent to comment on the functional dependence of Δp itself on the controlled, or uncontrolled, parameters of the experiment, and if this model is to have any interpretive value regarding the basic nature of the anomalous correlations with operator intention, some understanding of those relationships is essential. We know from the large databases of our hundreds of operators, especially the so-called “prolific” operators who have provided large individual databases, that if Δp is indeed the active factor, it is quite operator-specific.^(1,2) Beyond that, our prolific operators are known to evidence *long-term* changes in their individual effective Δp values, possibly associated with psychological aspects such as mood, style,

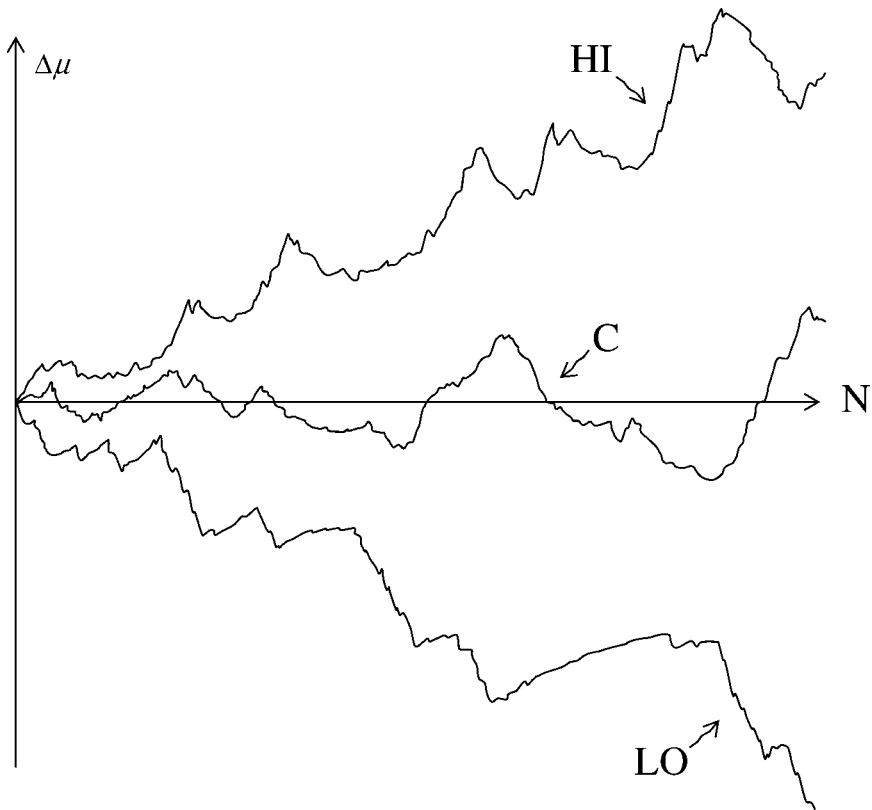


Fig. 1. Deviations of the output of an electronic random event generator from the theoretical chance mean as a function of the number of samples collected. Trace C: chance (calibration) behavior for $p = 0.5$. Trace HI: typical result of a “successful” high-intention experiment. Trace LO: typical result of a “successful” low-intention experiment.

health, novelty/boredom, maturation, *etc.* In contrast, the apparent variability in their individual and collective Δp values across experiments using different types of random devices as targets usually is less pronounced, suggesting that such a model is usefully ubiquitous, *i.e.*, relatively independent of technical details.

What is more problematic to assess, given the scale of the inherent noise of the random component of the data traces, is the degree of *shorter-term* variability in the Δp influence that may prevail in any given case. To the extent that this may be comparable with, or more rapid than, that of the intrinsic randomness of the output data, it would render such a feature useless, both conceptually and analytically. Only if the Δp values are relatively stable and capable of correlation with salient psychological or technical parameters does the concept retain much utility. The following analysis proceeds under the latter assumption, but is limited to just one such possible correlate which has both

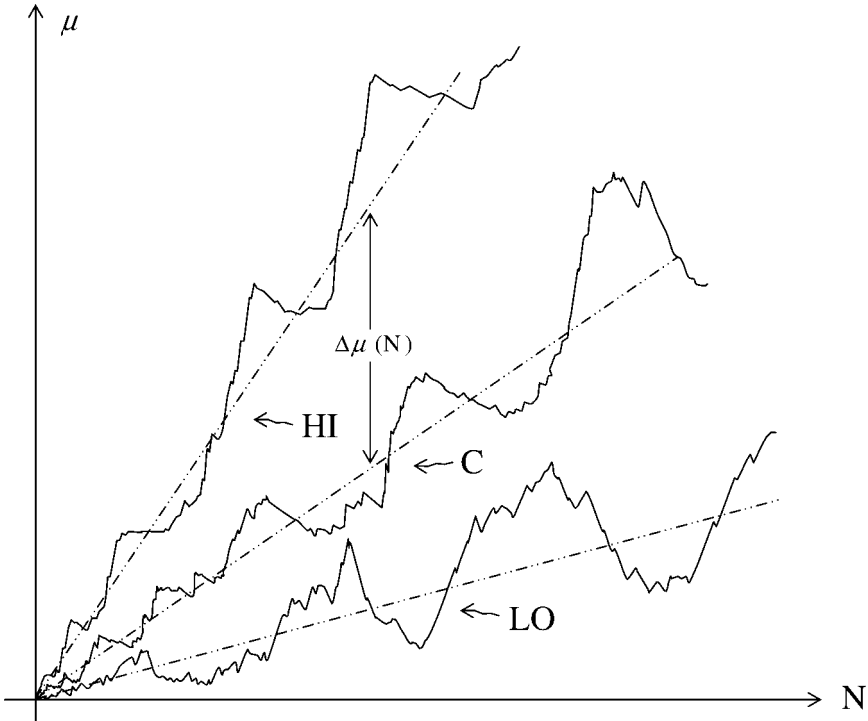


Fig. 2. Progression of overall mean values in a typical REG experiment. Trace C: chance behavior. Trace HI: successful high effort. Trace LO: successful low effort.

technical and psychological implications, namely the number of binary samples collected in a given experimental application.

II. Constant Effect Size

As alternatively sketched in Figure 2, trace C, the evolution of the performance of an ideally random binary source of constant $p = 0.5$ as a function of the number of samples collected entails a cumulative mean trace centered on $\mu_c = N/2$, embossed with a random component of amplitude characterized by a standard deviation growing as $\sigma_c = \sqrt{N/2}$. These two properties, μ and σ , completely define the output count distributions, and their quotient, $\mu_c/\sigma_c = \sqrt{N}$, in a sense represents the “signal-to-noise” ratio of the device.

Now, let us next assume that in a given active experiment the binary probability is changed by a constant amount, Δp , characteristic of that particular operator and his direction of intention (HI or LO), for that particular experiment, at that particular time. The corresponding course of the cumulative mean trace is now linearly displaced from the chance mean by an average amount $\Delta\mu(N) = \Delta pN$. (The difference between the new standard deviation and the chance value

is second order in Δp and can safely be neglected.) We also define as alternative statistical figures of merit an effect size \mathcal{E} and a Z-score given by

$$\mathcal{E} = \Delta\mu/\mu_c = 2\Delta p \quad (4)$$

$$Z = \Delta\mu/\sigma_c = \Delta p N/\sqrt{N}/2 = 2\Delta p\sqrt{N} = \mathcal{E}\sqrt{N}. \quad (5)$$

Note that while Δp and \mathcal{E} are linearly related and used more or less interchangeably in this analysis, the latter may be expressed in a variety of units, *e.g.*, bits/bit, bits/trial, bits/run, *etc.* Note also that if the prevailing binary probability (or average effect size) is independent of N , the average Z-score increases as \sqrt{N} . (This, of course, is the common premise that predicates the acquisition of large databases to escalate small, constant effect sizes to high statistical significance.)

III. Variable Effect Size

If, however, Δp is not constant over the given experiment, but is some function of the locally prevailing sample number, n , we must integrate this dependence to compute the cumulative mean shift, effect size, and Z-score up to the desired N , *i.e.*,

$$\Delta\mu_N = \int_0^N \Delta p(n) dn \quad (6)$$

$$\mathcal{E}_N = \left(\frac{\Delta\mu}{\mu_c}\right)_N = \frac{2}{N} \int_0^N \Delta p(n) dn \quad (7)$$

$$Z_N = \frac{\Delta\mu_N}{\sigma_c} = \frac{2\Delta\mu_N}{\sqrt{N}} = \frac{2}{\sqrt{N}} \int_0^N \Delta p(n) dn \quad (8)$$

where $\Delta\mu_N$, \mathcal{E}_N , and Z_N denote the values achieved at the completion of $n = N$. Obviously, if $\Delta p(n)$ is a constant over the span of N , we recover the previous results $\Delta\mu_N = \Delta p N$, $\mathcal{E}_N = 2\Delta p$, and $Z_N = 2\Delta p\sqrt{N}$, but for all other cases, the behavior of Z should be indicative of the profile of $p(n)$, again provided that $p(n)$ varies much more slowly than the stochastic noise of the system output.

For the balance of the discussion, let us assume that Δp is a monotonic function of n ; that is, that it only increases, or decreases, over the pertinent n -span of the given application. For example, if Δp increases linearly with n ,

$$\Delta\mu_N \propto \int_0^N n dn \propto N^2 \quad (9)$$

$$\mathcal{E}_N \propto \frac{\Delta\mu_N}{N} \propto N \quad (10)$$

$$Z_N \propto \left(\frac{\Delta\mu_N}{\sigma_c}\right)_N \propto N^{3/2}. \quad (11)$$

In contrast, if p decreases inversely with n ,

$$\Delta\mu_N \propto \ell n N \quad (12)$$

$$\mathcal{E}_N \propto \frac{\ell n N}{N} \quad (13)$$

$$Z_N \propto \frac{\ell n N}{\sqrt{N}}. \quad (14)$$

A particularly interesting special case is that for $\Delta p \propto 1/\sqrt{n}$, which yields

$$\Delta\mu_N \propto \sqrt{N} \quad (15)$$

$$\mathcal{E}_N \propto \frac{1}{\sqrt{N}} \quad (16)$$

$$Z_N = \text{const.} \quad (17)$$

This case calls to mind a number of empirical results and theoretical conceptualizations that have characterized the Princeton Engineering Anomalies Research (PEAR) REG research for many years. On the experimental side, there is the tendency of a number of individual and collective databases to yield Z -scores that digress from the parabolic increases $\propto \sqrt{N}$ predicted for constant Δp behaviors, toward asymptotic approaches to constant Z values, independent of N , with the associated declines in effect sizes.⁽⁶⁾

On the theoretical side, we have the informal testimony of some of our operators, and various conceptual speculations in some of our models, that it is the stochastic “noise” riding on the secular output “signals” of the target devices that provides the “raw material” out of which the anomalous deviations are created.⁽⁷⁾ If one ventures to identify as a quantitative index of this “available noise” the ratio of the prevailing standard deviation to the cumulative mean, the functional dependence of $\Delta p(n)$ conforms to this particular example, *i.e.*:

$$\Delta p(n) \propto \frac{\sigma(n)}{\mu(n)} \propto \frac{1}{\sqrt{n}}. \quad (18)$$

The corresponding hypothesis, then, is that as an operator proceeds to accumulate data in an REG experiment, the fraction of “available noise” or “intrinsic uncertainty” is decreasing, and with it his Δp ability, perhaps in accordance with the above relations. In other words, as the output signal, $\mu(n)$, becomes relatively cleaner with increasing n , the capacity for altering it deteriorates at a rate that allows no improvement in the Z -score, no matter how long, or how rapidly, the data are collected.

IV. Tests

A number of ways suggest themselves to search for the best empirical identification of the functional dependence of $\Delta p(n)$, utilizing retrospective

Table 1: Dependence of Effect Sizes, \mathcal{E} , on Run Lengths; Local, Benchmark Data⁽²⁾

91 Single Operators				
Trials/Run	BL	HI	LO	Δ
50	0.014 ± 1.283	3.181 ± 1.245	-2.349 ± 1.250	2.767 ± 0.882
100	2.184 ± 1.730	4.592 ± 1.730	-1.098 ± 1.730	2.845 ± 1.224
1000	2.081 ± 1.195	1.112 ± 1.195	-1.056 ± 1.195	1.084 ± 0.845
Operator A				
Trials/Run	BL	HI	LO	Δ
50	21.000 ± 9.129	-13.224 ± 9.285	-6.597 ± 8.980	-2.983 ± 6.455
100	0.050 ± 4.564	9.346 ± 4.564	-6.558 ± 4.564	7.952 ± 3.227
1000	4.213 ± 3.627	7.692 ± 3.627	-6.582 ± 3.627	7.137 ± 2.565
Operator B				
Trials/Run	BL	HI	LO	Δ
50	0.683 ± 2.661	7.767 ± 2.740	-6.968 ± 2.741	7.368 ± 1.938
100	-4.257 ± 4.226	13.367 ± 4.241	-5.465 ± 4.211	9.388 ± 2.988
1000	-0.235 ± 4.385	9.785 ± 4.385	-7.088 ± 4.385	8.437 ± 3.101

Notes: Effect sizes, $\mathcal{E} = 2\Delta p$, multiplied by 10^4 . Uncertainties reflect sizes of data sets.

analyses of the large 50-, 100-, and 1000-trial datasets that comprise our entire benchmark database.⁽²⁾ The most direct of these methods simply compares the overall effect sizes achieved by individual operators, or by entire groups of operators, on these three run lengths. Examples of these are shown in Table 1 for composite databases comprising all single, local operators who used more than one run length, and for two of our most prolific operators, here labeled A and B, individually. These values, of course, are averages over the run lengths, as well as over the full databases, but nonetheless should be indicative of any gross trends in $\Delta p(n)$. Graphical representations of these same data are presented in Figures 3 through 14. Here we have plotted the average effect sizes vs. the inverse square root of the run lengths, whereby the two options of $\Delta p = \text{const.}$ and $\Delta p \propto 1/\sqrt{n}$ present as families of horizontal lines and sloped lines through the origin, respectively. The best fits to the data for these two models, computed as least squares one-parameter linear regressions, are shown as dotted lines, to be compared with full two-parameter fits through the data, shown as solid lines. The most effective test for comparing the merits of these models is to compute the Z-score of each of these two parameters against zero.⁽⁸⁾ Since the constant-

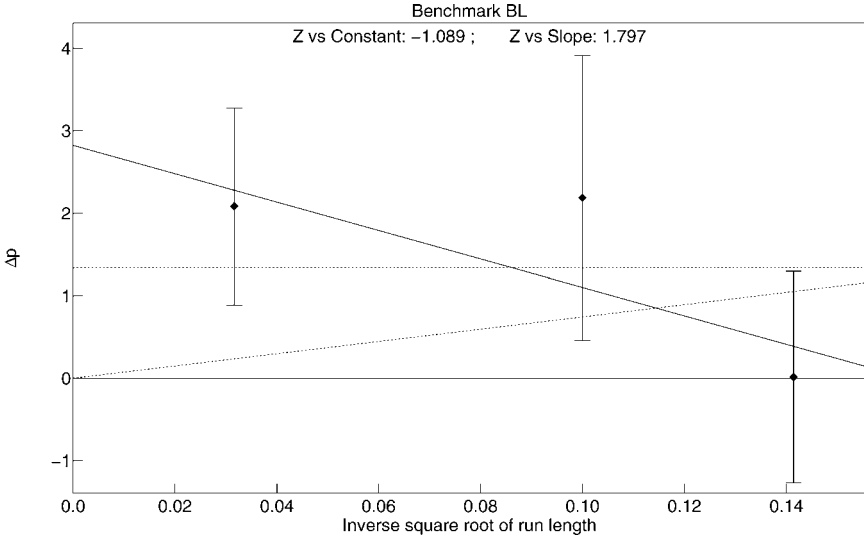


Fig. 3. Composite benchmark BL data. Shifts in binary probabilities, Δp , in units of 10^{-4} bits/bit, plotted vs. $1/\sqrt{N}$. Solid line: two-parameter (intercept and slope) linear regression least squares fit to data. Dotted lines: one-parameter fits to $\Delta p = \text{const.}$ (horizontal line) and $\Delta p \propto 1/\sqrt{N}$ (sloped line through origin) models. (Error bars reflect size of database. Z values reflect goodness of fits. See text.)

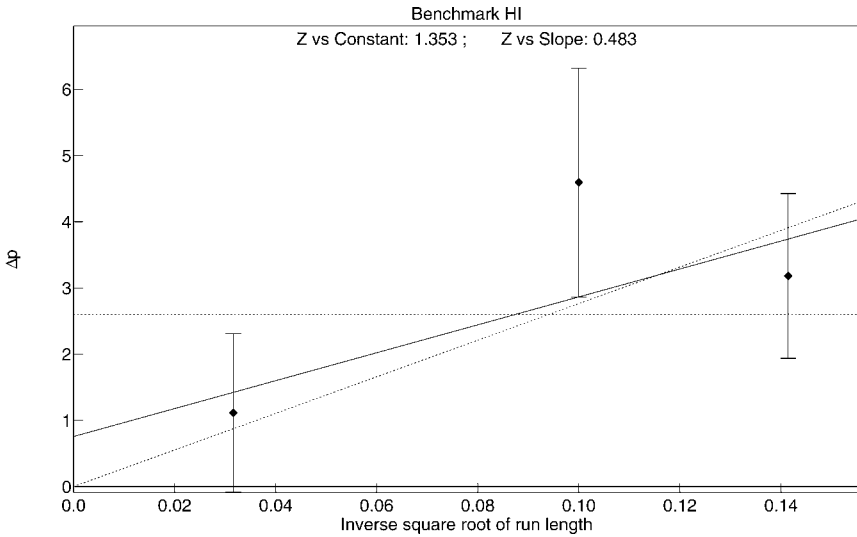


Fig. 4. Composite benchmark HI data. (See Figure 3 caption.)

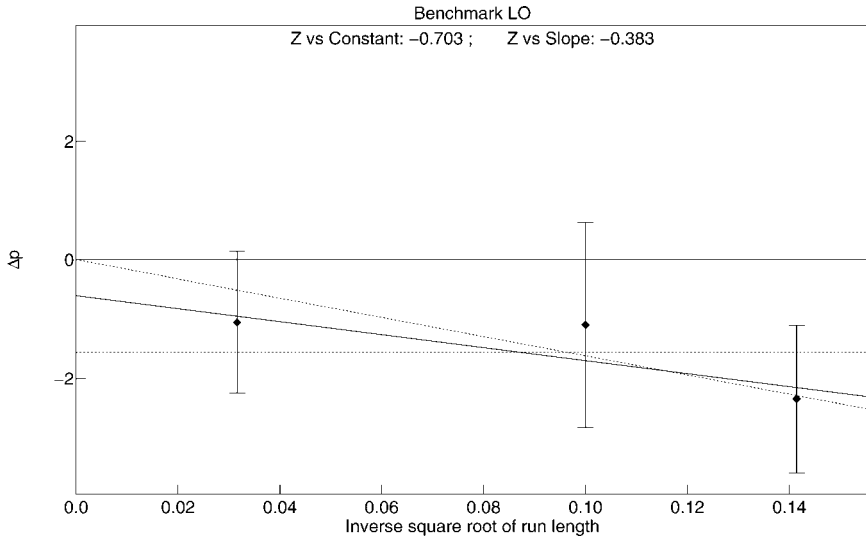
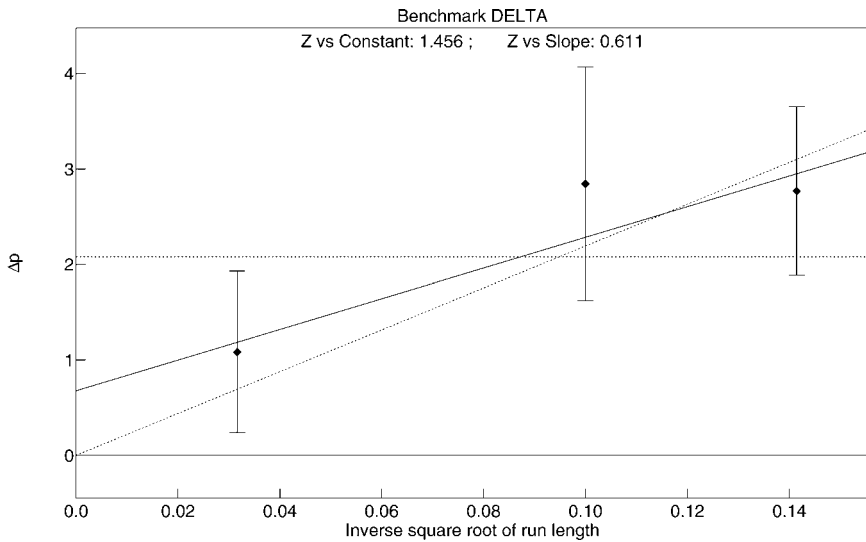


Fig. 5. Composite benchmark LO data. (See Figure 3 caption.)

Fig. 6. Composite benchmark Δ data. (See Figure 3 caption.)

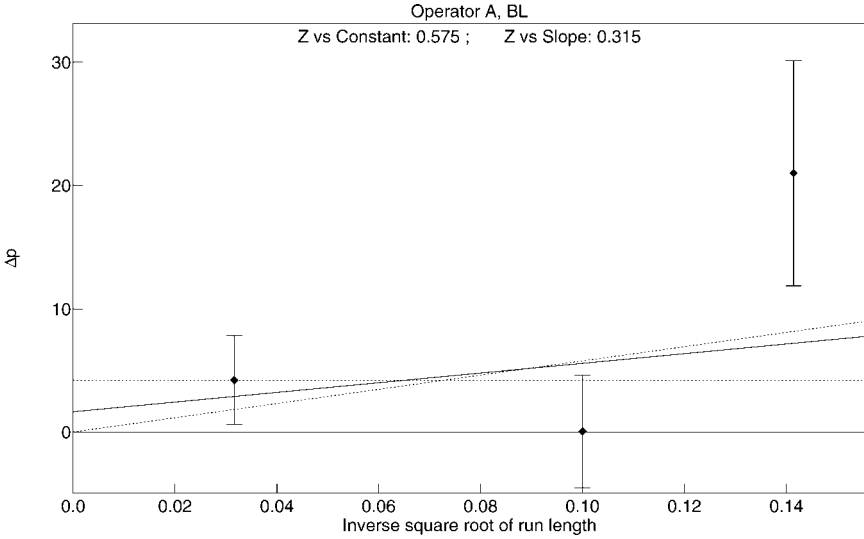


Fig. 7. Operator A—BL data. (See Figure 3 caption.)

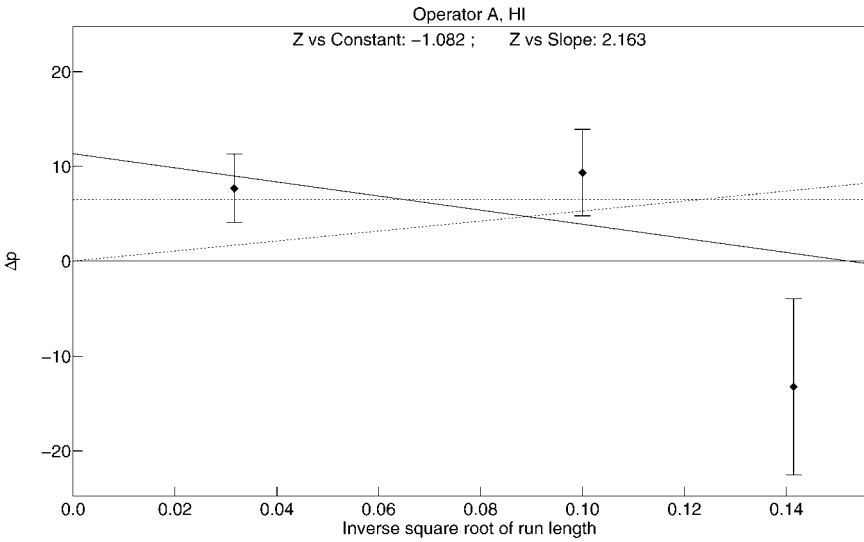


Fig. 8. Operator A—HI data. (See Figure 3 caption.)

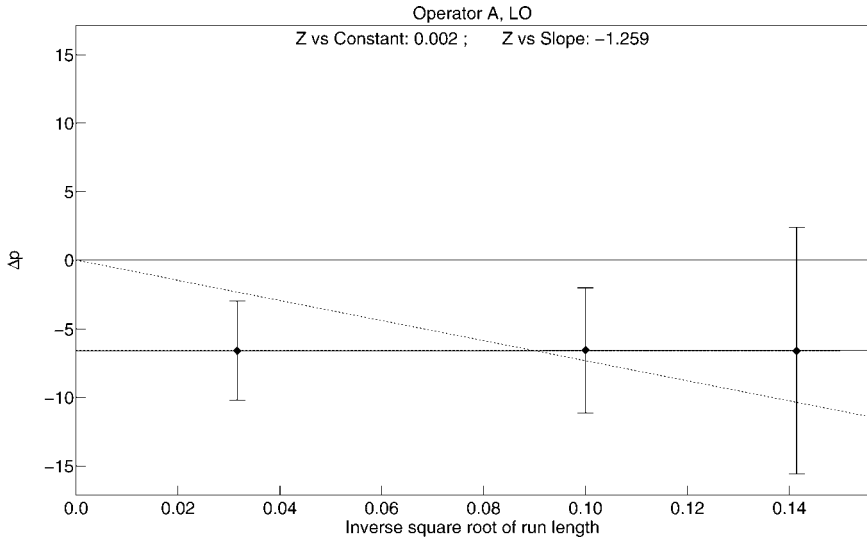


Fig. 9. Operator A—LO data. (See Figure 3 caption.)

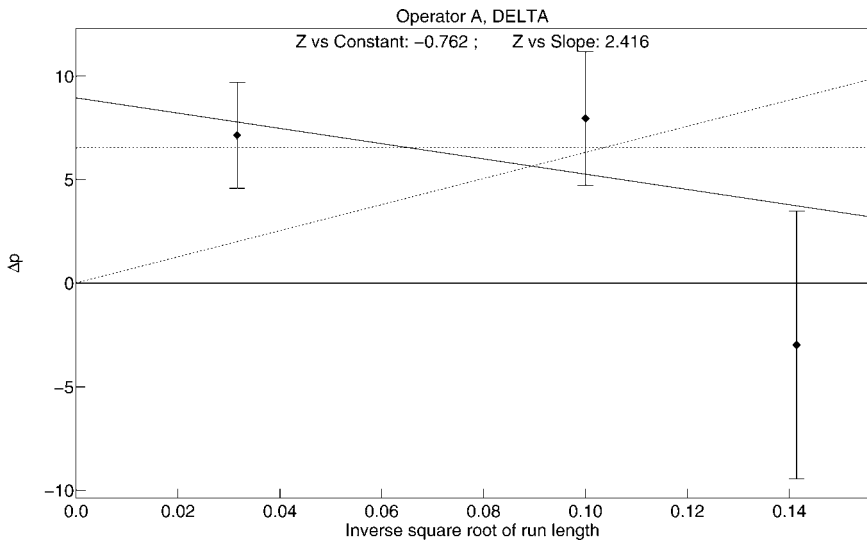


Fig. 10. Operator A— Δ data. (See Figure 3 caption.)

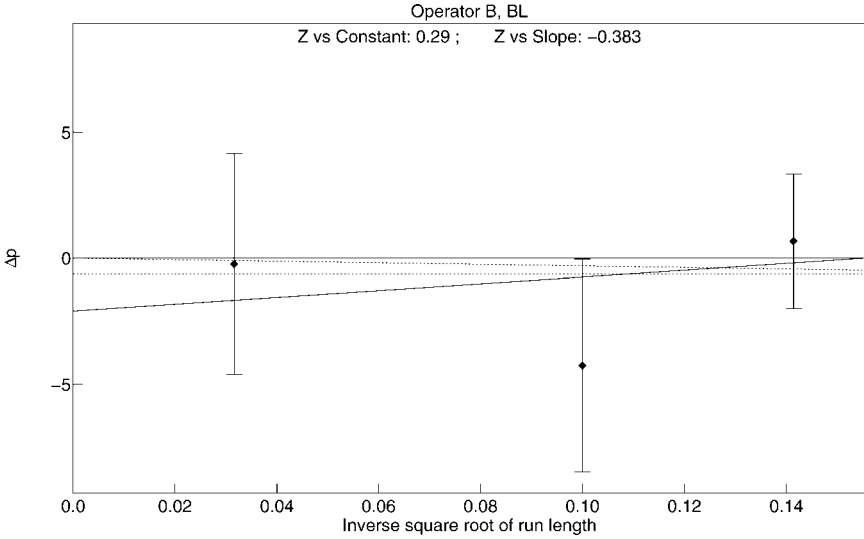


Fig. 11. Operator B—BL data. (See Figure 3 caption.)

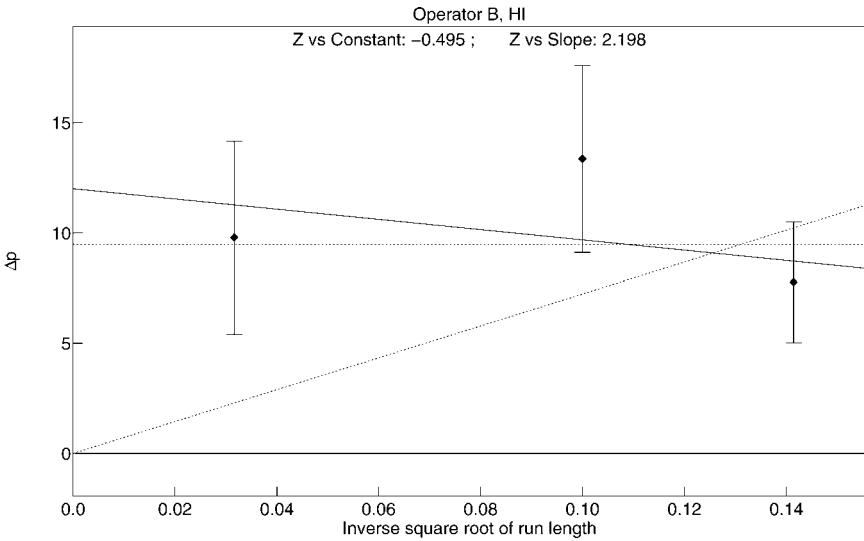


Fig. 12. Operator B—HI data. (See Figure 3 caption.)

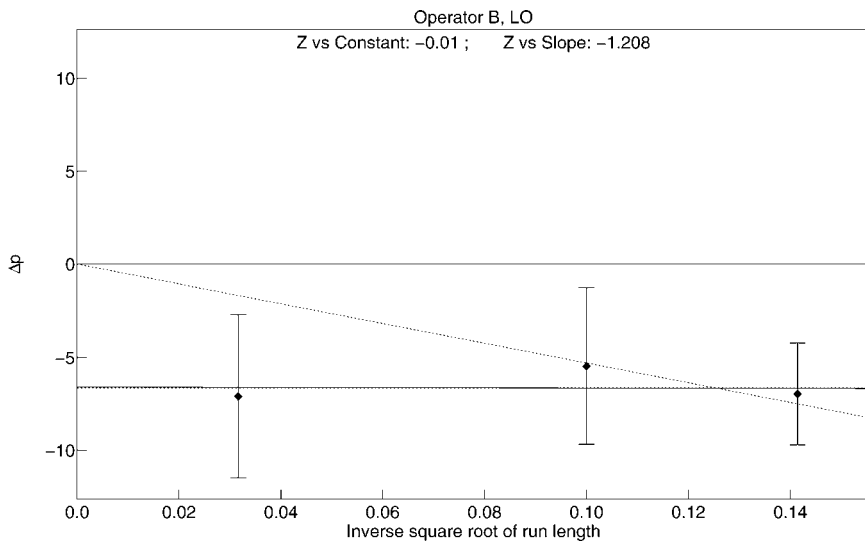
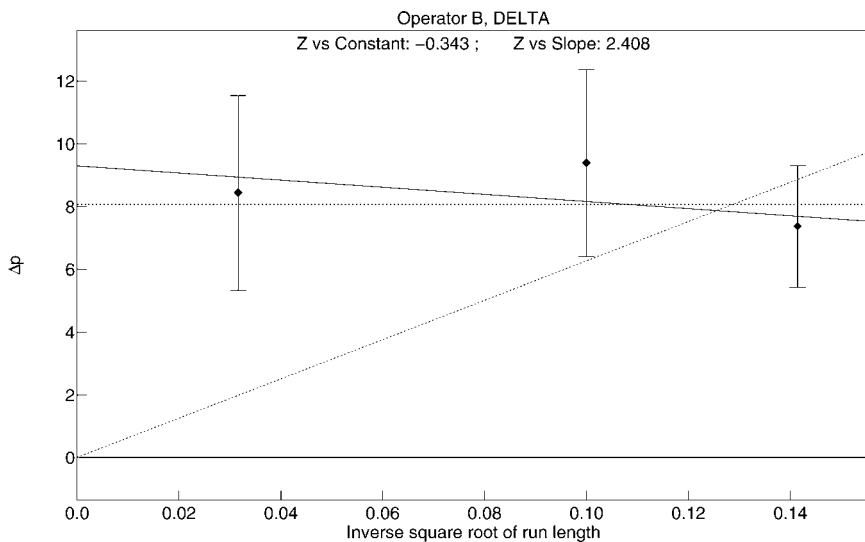


Fig. 13. Operator B—LO data. (See Figure 3 caption.)

Fig. 14. Operator B— Δ data. (See Figure 3 caption.)

effect model requires the linear fits to have zero slope, the Z -score of the data's regression slope, against the zero value required by the model, is a Z -score against the hypothesis that the data contain a constant effect; large values of this Z refute this model. Likewise, since the $\Delta p \propto 1/\sqrt{n}$ model is in this representation a linear fit that must pass through the origin, the Z -score of the data regression intercept value is the appropriate Z against the hypothesis that the effect declines as $1/\sqrt{n}$.

Looking first at the baseline data for the composite database (Figure 3), we find little discrimination between these two models, as would be expected for these small effect sizes. For the HI data (Figure 4), there appears a marginal preference for the $\Delta p \propto 1/\sqrt{n}$ model, and similarly, but even less so, for the LO data (Figure 5). These compound to a Δ behavior (Figure 6) which shows a bit larger tendency to the same model, but still insignificantly so.

On the argument that these data are badly diluted by the large fraction of "unsuccessful" performances included in the composite database, we then turn to individual data from two of our most successful operators to search for better discriminations between these two Δp options. For operator A we again find little distinction in the baseline or HI data (Figures 7 & 8), but some preference in the LO and Δ for the constant Δp model (Figures 9 & 10). Only in operator B data do we find statistically significant discriminations in favor of the constant Δp model, in both the HI and Δ groupings (Figures 12 & 14).

A more sophisticated approach entails breaking the three run-length sets into 50-trial segments, *i.e.*, one segment for all 50-trial runs, two segments for all 100-trial runs, and 20 segments for all 1000-trial runs, and plotting the corresponding effect sizes *vs.* the ordinal number of the segments. Figures 15 through 18 show such graphs for the baseline (BL), high (HI), low (LO), and high minus low (Δ) data for the full benchmark database. These data can then also be subjected to a least squares fit against any functional model of $\Delta p(n)$. Superimposed on the figures are the best such fits against the two models $\Delta p = \text{const.}$ and $\Delta p \propto 1/\sqrt{n}$. It is quite evident from casual inspection of these figures that even this more comprehensive treatment lacks the statistical power to distinguish clearly between the two models. To confirm this quantitatively, the plotted data may be compared with both of the best-fit model predictions to generate a chi-squared (χ^2) value for the residual variations from these models. These χ^2 values, their degrees of freedom, and their associated chance probabilities are listed in Table 2. In contrast to the BL data, it appears that the HI, LO, and Δ data all entail somewhat *less* variation than expected by chance for both of the models, but as anticipated, the two models appear equally good; *i.e.*, the data cannot distinguish between them.

It could again be posited that the discrimination we seek is being obscured by the internal vagaries of this large database, *e.g.* by the vast disparities in individual operator performance, dataset sizes, personal preferences for particular run lengths, *etc.* For this reason, it again seems worthwhile to

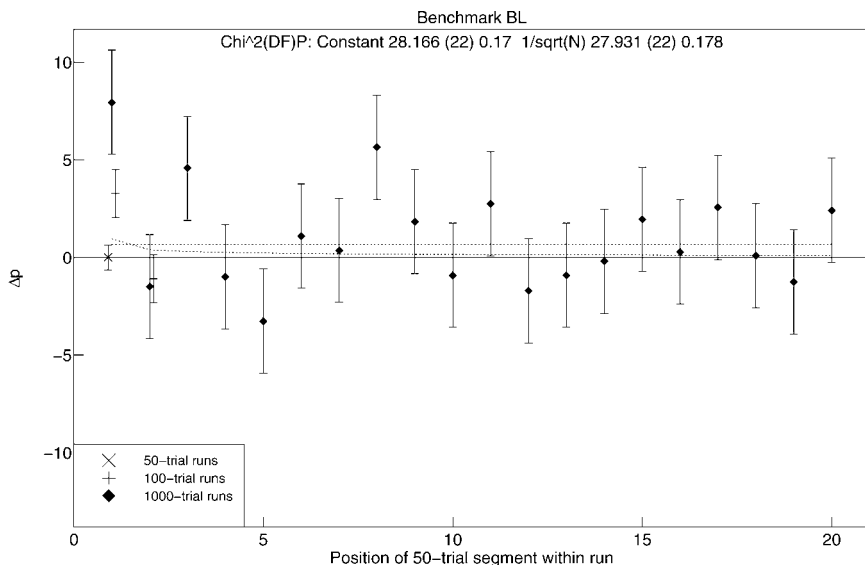


Fig. 15. Composite benchmark BL data. Evolution of binary probability shifts, Δp , as a function of N within runs, compared with $\Delta p = \text{const.}$ (horizontal dotted line) and $\Delta p \propto 1/\sqrt{N}$ (dotted curve) models. (See text.)

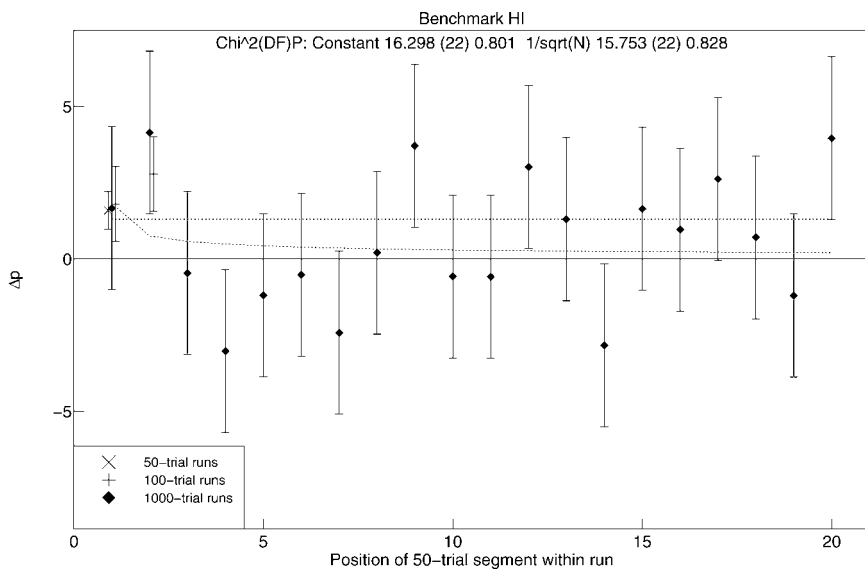


Fig. 16. Composite benchmark HI data. (See Figure 15 caption.)

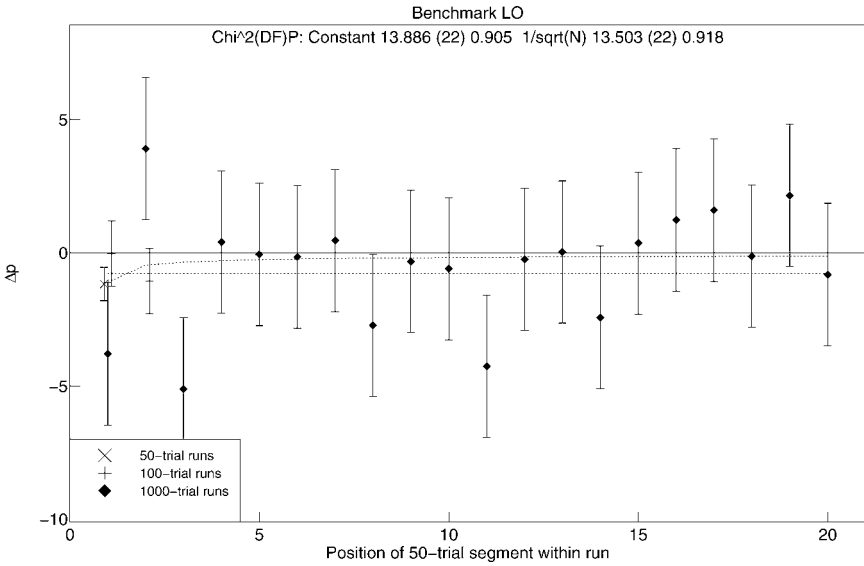


Fig. 17. Composite benchmark LO data. (See Figure 15 caption.)

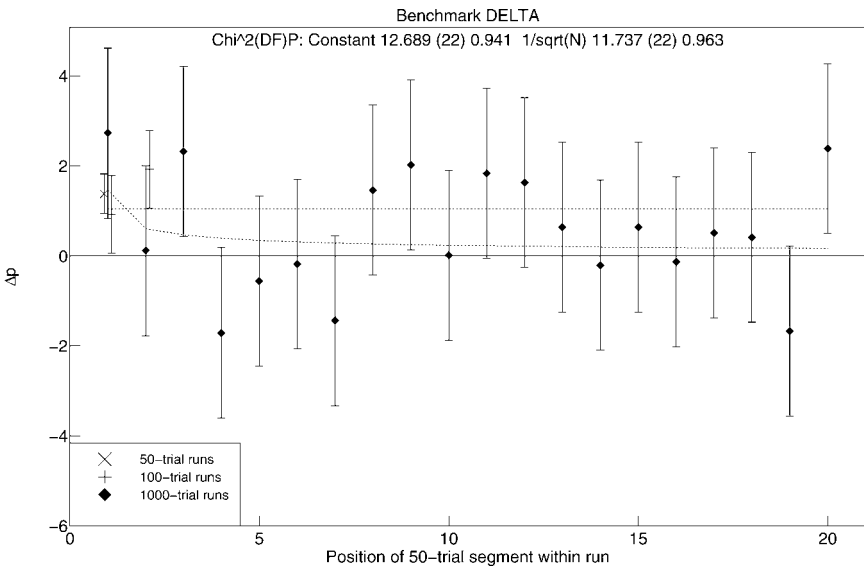


Fig. 18. Composite benchmark Δ (HI - LO) data. (See Figure 15 caption.)

**Table 2: Effect Evolution As a Function of n within Runs:
Local, Benchmark Data:⁽²⁾**

χ^2 Values of 50-Trial Segments of 50-, 100-, and 1000-Trial Runs
vs. $\Delta p = \text{const.}$ and $\Delta p = \text{const.}/\sqrt{n}$ Best-Fit Models

91 Single Operators				
	BL	HI	LO	Δ
χ^2 vs. $\Delta p = k$ (p_χ)	28.17 (0.17)	16.30 (0.80)	13.89 (0.91)	12.69 (0.94)
χ^2 vs. $\Delta p = k/\sqrt{n}$ (p_χ)	27.93 (0.18)	15.75 (0.83)	13.50 (0.92)	11.74 (0.96)
Operator A				
χ^2 vs. $\Delta p = k$ (p_χ)	24.03 (0.35)	15.90 (0.82)	14.51 (0.88)	11.06 (0.97)
χ^2 vs. $\Delta p = k/\sqrt{n}$ (p_χ)	24.06 (0.34)	19.72 (0.60)	14.67 (0.88)	15.55 (0.83)
Operator B				
χ^2 vs. $\Delta p = k$ (p_χ)	27.16 (0.21)	19.14 (0.64)	14.14 (0.90)	19.26 (0.63)
χ^2 vs. $\Delta p = k/\sqrt{n}$ (p_χ)	27.16 (0.21)	25.13 (0.29)	17.15 (0.76)	28.00 (0.18)

Notes: All χ^2 have 22 degrees of freedom. χ^2 probabilities (p_χ) > 0.50 connote better fits than average chance expectations.

examine individually the data from two of the most successful prolific operators, to see whether a particular $\Delta p(n)$ preference emerges at that level. Figures 19 through 26 and Table 2 show the corresponding graphical treatments and χ^2 tabulations for the two operators used above, again labeled A and B. The former displays behavior similar to that of the composite database with intentional results a bit too-closely configured to both of the models. The latter, however,

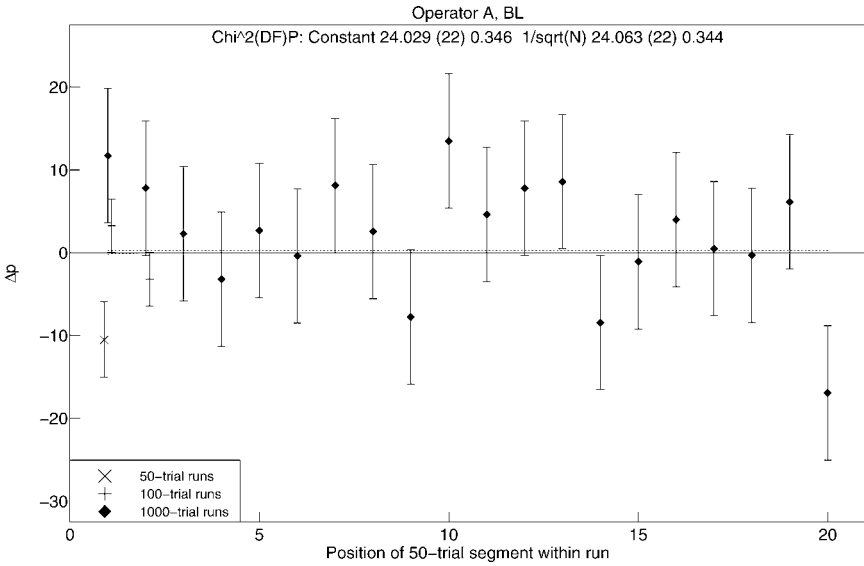


Fig. 19. Operator A—BL data. (See Figure 15 caption.)

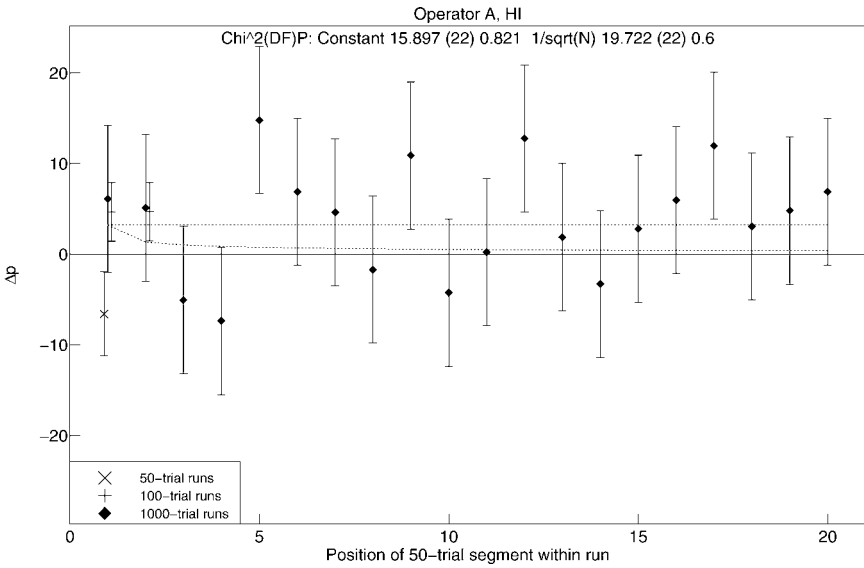


Fig. 20. Operator A—HI data. (See Figure 15 caption.)

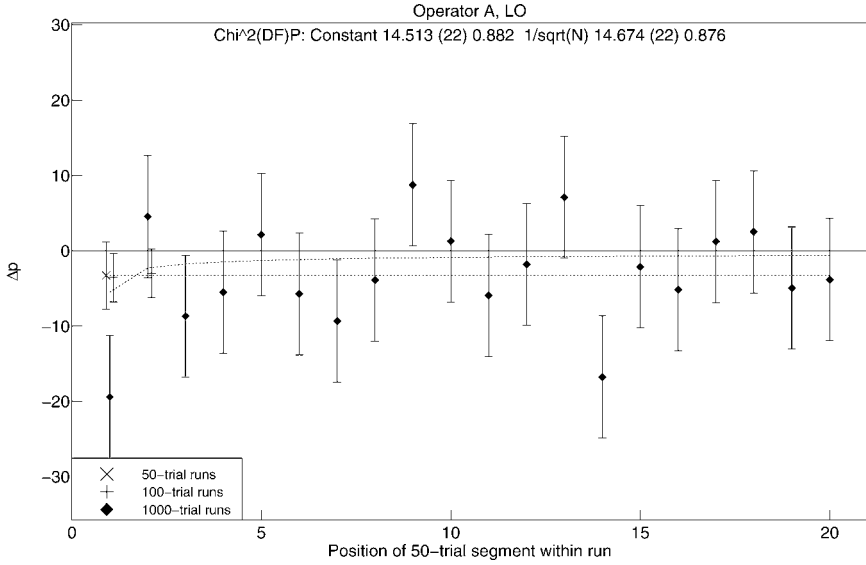


Fig. 21. Operator A—LO data. (See Figure 15 caption.)

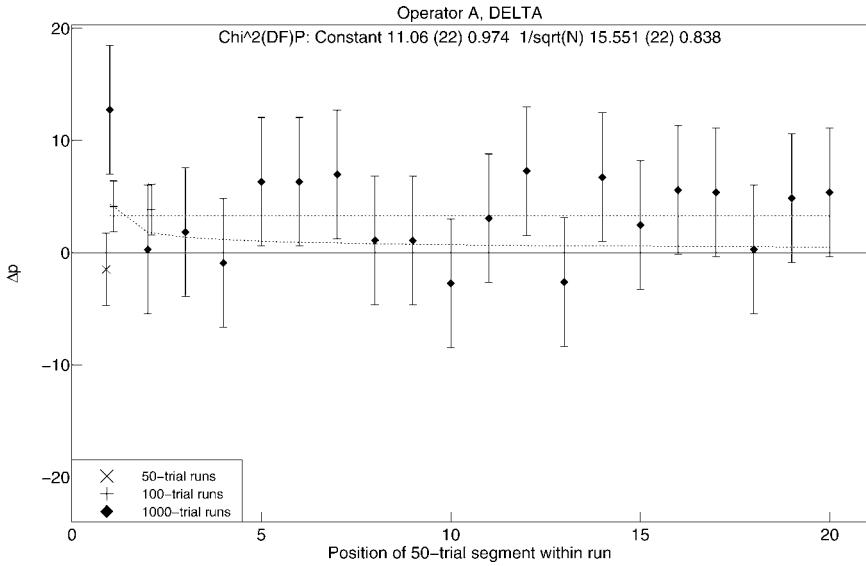


Fig. 22. Operator A— Δ data. (See Figure 15 caption.)

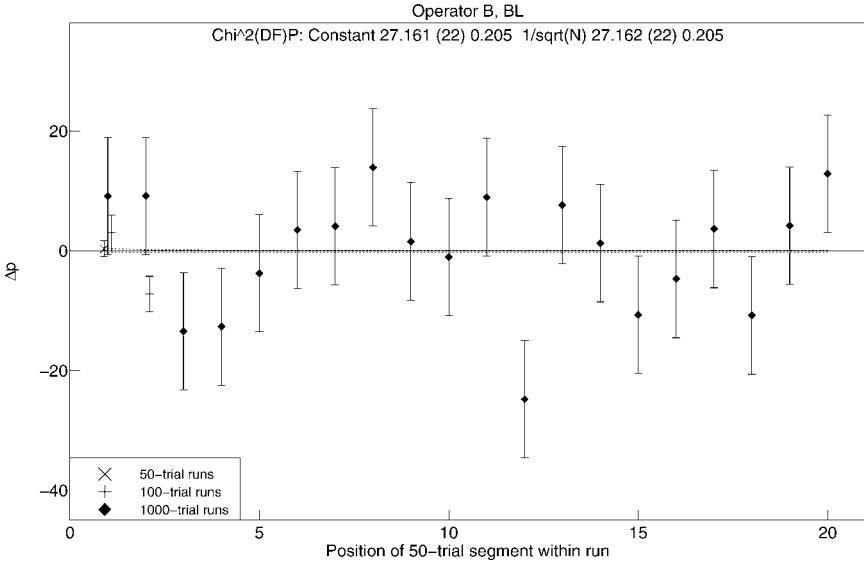


Fig. 23. Operator B—BL data. (See Figure 15 caption.)

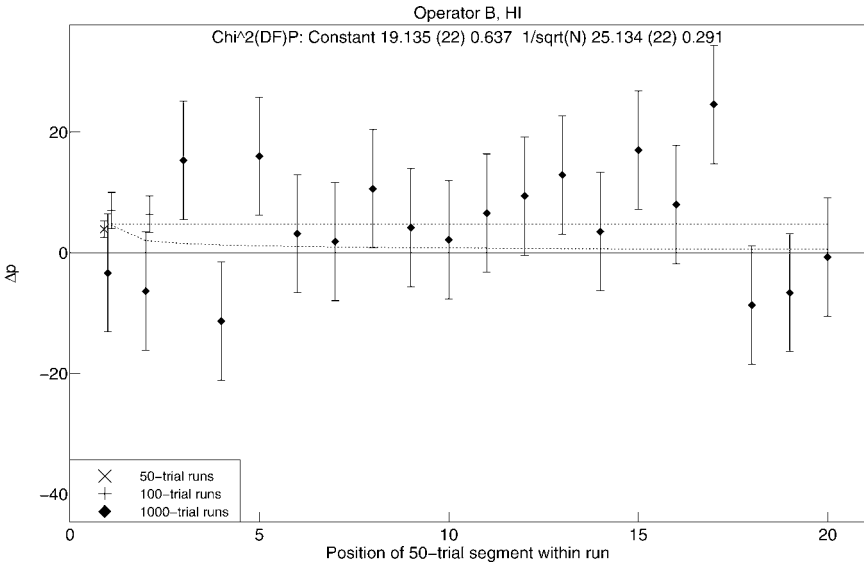


Fig. 24. Operator B—HI data. (See Figure 15 caption.)

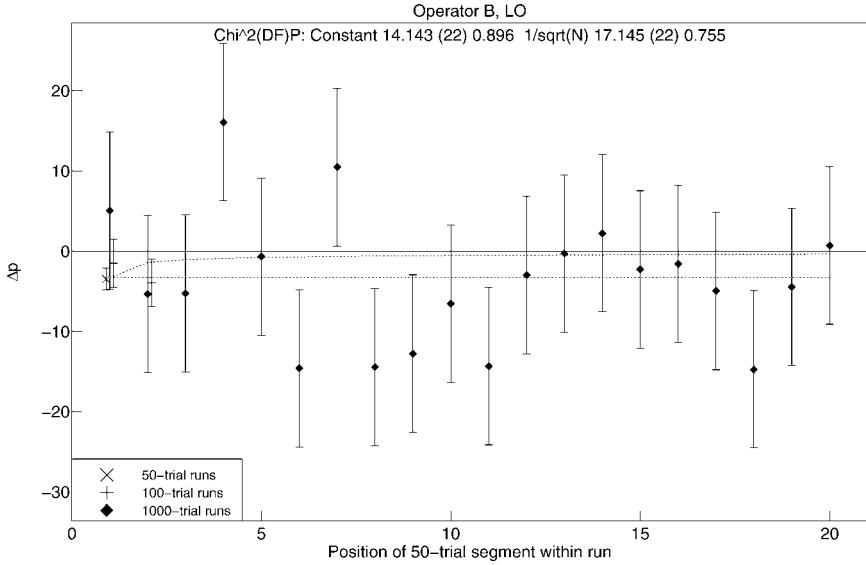


Fig. 25. Operator B—LO data. (See Figure 15 caption.)

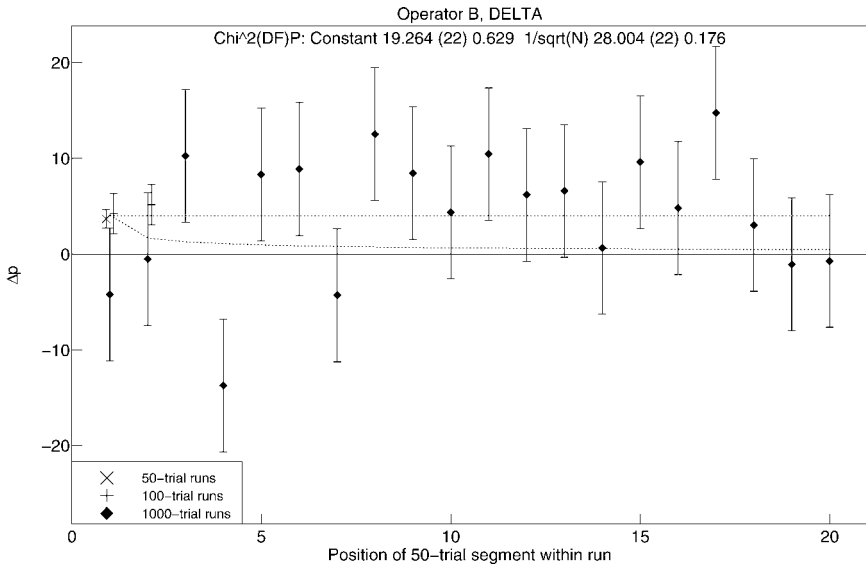


Fig. 26. Operator B— Δ data. (See Figure 15 caption.)

again shows some preference, albeit not statistically significant, in both the HI and Δp data, for the constant Δp model.

V. Discussion

From these and many other data not presented here, it thus appears that the hypothesis of an effect size driven by the local “noise-to-signal ratio” (or, more technically, the “cumulative proportional uncertainty”) as defined by the σ/μ criterion, cannot be sustained. Rather, at least in the case of operator B, it is the constant Δp model that better fits the data, albeit marginally so. It is possible, of course, that the technical ratio σ/μ is not the pertinent specification of noise/signal in the psychological context. For example, if it were the ratio of the *variance*, σ^2 , of the output data stream to the developing mean value, $\mu(n)$, that conditioned the Δp capability, then this index, and its corresponding effect size, would be independent of n , and we could no longer even attempt to distinguish this model from any other constant Δp version.

Alternatively, one could speculate that the proper specification of the “signal” factor in the noise-to-signal ratio is not the cumulative mean, $\mu(n)$, but the cumulative mean shift, $\Delta\mu(n)$, which serves as “signal” in the ratio, *i.e.*, $\Delta p \propto \sigma/\Delta\mu$. This, of course, introduces a non-linearity into the loop, *e.g.*,

$$d(\Delta\mu) = \Delta p \, dn \propto \frac{\sigma}{\Delta\mu} \, dn \quad (19)$$

$$d(\Delta\mu)^2 \propto \sigma \, dn \quad (20)$$

$$\Delta\mu \propto \sqrt{\sigma n} \propto n^{3/4} \quad (21)$$

$$\Delta p \propto n^{-1/4}. \quad (22)$$

Similarly, it could be the gradient, $d\mu/dn$, that the operator utilizes as “signal.” For any constant Δp process, this derivative is also constant, and the argument does not change. But if $\Delta p(n)$ is not constant, neither is $d\mu/dn$, and the problem again becomes non-linear, *e.g.*,

$$\Delta p(n) \propto \left(\frac{\sigma}{d\mu/dn} \right) \propto \left(\frac{\sqrt{n}}{\Delta p(n)} \right) \quad (23)$$

$$\Delta p(n) \propto n^{1/4}. \quad (24)$$

Unfortunately, the data available are even less likely to distinguish such weak dependencies from a constant Δp version.

There is a somewhat subtler argument that might be advanced for the failure of any of the above “noise/signal” models to capture the Δp -altering mechanism suggested by the operator self-reports, namely, that it is not the technical noise level, *per se*, but the subjective *uncertainty* experienced by the operators that is the salient factor in feeding the anomalous effect, and that attempting to specify

or quantify this by any measure derived from the objective data streams excludes all of the subjective factors that may contribute to this uncertainty reservoir. (A similar possibility emerged from a detailed remote perception study published previously,⁽⁷⁾ and a theoretical attempt to deal with this class of omission has been presented by Atmanspacher⁽⁹⁾.)

Setting aside the failure to identify any convincing departures from a constant Δp model in the collective or individual databases, there remains to note the oddly small χ^2 deviations in the collective and individual datasets, in nearly all of the HI, LO, and Δ intentions, compared with their more expected behavior in the baseline data (*cf.* Table 2). Most simply summarized, it appears that whatever average values of Δp prevail in those datasets, their block-wise variations are marginally smaller than expected even for the *displaced* chance distributions, *i.e.*, the block-wise variance in the prevailing Δp values are suggestively small or, alternatively, there is some degree of correlation among them. It is not clear that this behavior is real, since its statistical significance is modest and it is observed retrospectively. At most, it is a signal that similar experiments should be monitored for like suppression of variance. If real, this implies that the anomalous mean shift entails, or at least is accompanied by, behavior incompatible with simple probability shifts in the data; these can increase variation or leave it unchanged but cannot reduce it. At the very least, reducing the variation between samples requires a probability shift that is adaptive and exhibits negative feedback, so that it is weaker in runs where the spontaneous random variations are favorable, but stronger in runs where such variation is unfavorable. Alternatively, the anomalous mean shift may be accompanied by the imposition of autocorrelation as a side effect, or even accomplished by the controlled imposition of autocorrelation. Still other models can be proposed, the sole common feature being that some sort of time-dependence and/or state-dependence in the anomalous response must appear. Current data are far from adequate for distinguishing among these hypotheses. As suggested above, definitive empirical tests must await data comparisons with other REG-based experiments. In addition to the small χ^2 values, the traces in several of Figures 15 through 26 give some impression of temporally structured, nonmonotonic variations. Evaluation of these will require application of harmonic analyses suitable for assessing the general temporal evolution of such datasets.

Acknowledgments

The authors are indebted to Brenda Dunne for the original suggestion of such Δp dependencies, and to the multitude of operators who have provided the data on which the analyses are based. Lisa Langelier-Marks and Elissa Hoeger helped with preparation of the manuscript.

Financial support for the Princeton Engineering Anomalies Research laboratory has been provided by generous contributions from the Institut für Grenzgebiete der Psychologie und Psychohygiene; The Lifebridge Foundation;

The Center for the Science of Life; Richard Adams; George Ohrstrom; Laurance Rockefeller; and numerous other private contributors who prefer to remain anonymous.

References

- ¹ Jahn, R. G., Dunne, B. J., & Nelson, R. D. (1987). "Engineering anomalies research." *Journal of Scientific Exploration* 1, No. 1, pp. 21–50.
- ² Jahn, R. G., Dunne, B. J., Nelson, R. D., Dobyns, Y. H., & Bradish, G. J. (1997). "Correlations of random binary sequences with pre-stated operator intention: A review of a 12-year program." *Journal of Scientific Exploration* 11, No. 3, pp. 345–367.
- ³ Dunne, B. J. (1998). "Gender differences in human/machine anomalies." *Journal of Scientific Exploration* 12, No. 1, 3–55.
- ⁴ Jahn, R. G., & Dunne, B. J. (1988). *Margins of Reality: The role of consciousness in the physical world*. New York: Harper Brace Jovanovich.
- ⁵ Jahn, R. G., Dobyns, Y. H., & Dunne, B. J. (1991). "Count population profiles in engineering anomalies experiments." *Journal of Scientific Exploration* 5, No. 2, pp. 205–232.
- ⁶ Dunne, B. J., Dobyns, Y. H., Jahn, R. G., & Nelson, R. D. (1994). "Series position effects in random event generator experiments, with appendix by Angela Thompson." *Journal of Scientific Exploration* 8, No. 2, pp. 197–215.
- ⁷ Dunne, B. J., & Jahn, R. G. (2003). "Information and uncertainty: 25 years of remote perception research." *Journal of Scientific Exploration* 17, No. 2, pp. 207–241.
- ⁸ Dobyns, Y. H. (2000). "Overview of several theoretical models on PEAR data." *Journal of Scientific Exploration* 14, No. 2, pp. 163–194.
- ⁹ Atmanspacher, H. (2003). "Mind and matter as asymptotically disjoint, inequivalent representations with broken time-reversal symmetry." *BioSystems* 68, pp. 19–30.